

# Chitosan Supported Palladium Catalyst. VI. Nitroaniline Degradation

Thierry Vincent, Francisco Peirano, Eric Guibal

*Ecole des Mines d'Alès, Laboratoire Génie de l'Environnement Industriel, 6 avenue de Clavières, F-30319 Alès cedex, France*

Received 9 February 2004; accepted 17 May 2004

DOI 10.1002/app.21051

Published online in Wiley InterScience (www.interscience.wiley.com).

**ABSTRACT:** A chitosan-supported palladium catalyst was prepared by immobilization of palladium on glutaraldehyde crosslinked chitosan followed by in situ chemical reduction. This catalyst was successfully used for the degradation of 4-nitroaniline (4-NA) in the presence of sodium formate, used as the hydrogen donor. The reaction product was 1,4-phenylenediamine. The degradation was favored by acidic pH. A 10 to 15 excess of formate (compared to 4-NA) is required to achieve complete degradation of the substrate.

The reaction appears to be limited to the external layers of the catalyst: small particle size is required to optimize the degradation kinetics. Alternatively, an increase of catalyst dosage is required to increase kinetic rates but at the expense of palladium consumption. © 2004 Wiley Periodicals, Inc. *J Appl Polym Sci* 94: 1634–1642, 2004

**Key words:** chitosan; catalysis; palladium; nitroaniline degradation; pH; kinetics

## INTRODUCTION

Nitroaromatic compounds and their reduction products are frequently found in wastewater and soils as a result of the manufacture of many explosive materials (such as trinitrotoluene).<sup>1</sup> Due to their toxic and mutagenic impact, even at very low concentration, many processes have been developed to recover them from dilute solutions. Adsorption processes have been developed using, for example, polymers.<sup>1</sup> However, there is increasing interest in the development of degradation processes that avoid the simple transfer of the pollutant from a disperse medium to a controlled phase (as occurs with adsorption processes). Biological processes have been developed but they require very strict control of experimental conditions. Catalytic and photocatalytic processes are frequently cited as a promising alternative to conventional treatments.<sup>2,3</sup> Although homogeneous catalysis remains widely used in the chemical industry, the cost of some catalytic metals (such as platinum group metals) and/or metal complexes has increased the interest in developing supported catalysis. Supported-catalysis facilitates recovery of the metal after chemical reaction. Mineral materials (silica, alumina, zeolites)<sup>4,5</sup> and activated carbon are frequently used to support catalytic metals.<sup>6,7</sup> Polymeric supports have recently received a great deal of attention.<sup>8</sup> Indeed, the structure

of the polymer can provide additional advantages such as enantioselectivity.<sup>9–11</sup> Hence, the supplementary cost of specially tailored polymers can be compensated by very important additional properties, especially in the field of chemical synthesis. Orientation of the reaction toward the synthesis of preferred species increases the interest in a given reaction. Indeed, the stereospecific properties of these materials are able to improve the selectivity of the reaction.<sup>9,11–14</sup>

Polymer-supported catalysis has mainly been developed using synthetic polymers.<sup>8–11,13</sup> However, there is increasing interest in the use of natural polymers. These biopolymers are frequently characterized by highly enantioselective properties and have been used for chiral separation.<sup>15–19</sup> Moreover, these supports come from renewable resources and are usually cheaper than supports such as zeolite that require elaborate production processes. For these reasons many studies have recently focused on using biopolymers such as chitosan.<sup>20–28</sup> The high affinity of chitosan for metal ions is another important reason that helps to explain this increasing interest in chitosan as a support for heterogeneous catalysis. Chitosan, produced by the alkaline deacetylation of chitin, the most abundant polymer in nature, is made up of glucosamine and acetylglucosamine units. The polymer is characterized by a high percentage of amine functions, which are very reactive with metal ions, involving such different mechanisms as chelation for metal cations in near-neutral solutions and ion exchange for metal anions in acidic solutions.

For example, in the case of precious metals such as gold, palladium, or platinum, sorption capacities as

Correspondence to: E. Guibal (Eric.Guibal@ema.fr).

high as 1–2 mmol metal  $\text{g}^{-1}$  can be reached with chitosan that has simply been crosslinked (to avoid the polymer dissolving in acidic solutions).<sup>29,30</sup> In the case of other metals, the sorption capacity can reach levels as high as 7–8 mmol metal  $\text{g}^{-1}$  (for example for molybdate or vanadate sorption).<sup>31,32</sup> While some of these metals can easily be desorbed by pH variation (alkaline desorption for metal anions, and acid desorption for metal cations), others are strongly bound to the biopolymer. Above pH 1, the amounts of palladium and platinum that can be desorbed do not exceed a few percent. The precious metals thus remain stable on the catalyst. These catalysts are also environmentally friendly since, at the end of the life cycle, the polymer can be thermally degraded to recover precious metals with minimum contamination effect compared to some common resins and polymers.

We had previously designed chitosan-supported palladium catalyst for the reduction of chromate in dilute solutions<sup>26</sup> and more recently for the dehalogenation of chlorophenol<sup>33</sup> and degradation of nitrophenol.<sup>34</sup> The preparation of the support consists of a two-step procedure: (a) first, sorption of the precious metal on the previously conditioned polymer (to avoid the polymer dissolving), followed by (b) chemical reduction of the metal immobilized on the biopolymer.<sup>26</sup> The chromate reduction, chlorophenol dehalogenation, and nitrophenol degradation were performed using sodium formate as the electron or hydrogen donor. The procedure for catalyst preparation described in this study allowed the use of sodium formate while the procedure described in other recent papers, using palladium deposited on chitosan in alcoholic medium (and subsequent reduction in alcoholic medium),<sup>24</sup> was revealed to be inefficient for the target reaction using sodium formate (unpublished results). The use of hydrogen gas as the hydrogen donor is an alternative process (currently under investigation) that is expected to facilitate practical application and improve kinetic regulation, although the reaction can be controlled by the hydrogen solubility in water and by the exchange surface area between gas phase and liquid phase (using thin hollow fibers with high external surface area is of great interest when using hydrogen gas). Hydrogen gas has also been successfully used for hydrogen transfer reaction in the degradation of nitrophenol.<sup>35</sup>

The present work focuses on the degradation of 4-nitroaniline using a palladium catalyst immobilized on chitosan. In this study sodium formate has been used as the hydrogen donor; however, recent investigations showed that other hydrogen donors can be used including hydrogen gas, sodium borohydride, or hydrazine (unpublished results). The influence of several parameters on nitroaniline degradation kinetics and conversion yield was tested: pH, sodium formate concentration, nitroaniline concentration, catalyst dos-

age (CD), catalyst particle size (PS). Previous experiments on nitrophenol degradation confirmed that agitation speed hardly influenced degradation kinetics.<sup>34</sup>

## METHODS

### Materials

Chitosan was supplied by Aber Technologies (Plouvien, France). It was previously characterized.<sup>29</sup> The degree of deacetylation is 87% and the molecular weight is  $125,000 \text{ g mol}^{-1}$ . Chitosan was ground and sieved to separate it into samples of different particle sizes:  $0 < \text{PS1} < 125 \mu\text{m} < \text{PS2} < 250 \mu\text{m} < \text{PS3} < 500 \mu\text{m} < \text{PS4} < 710 \mu\text{m}$ . Another sample (PS0) was prepared by grinding the PS1 fraction and sieving the final powder to select the 0- to 63- $\mu\text{m}$ -size fraction.

4-Nitroaniline was purchased from Fluka (Switzerland) as an analytical grade product.  $\text{PdCl}_2$  was purchased from Acros. Other reagents (acids, zinc,  $\text{HCOONa}$ ) were supplied by Carlo Erba (Italy).

### Sorbent preparation

Since chitosan is soluble in hydrochloric acid it cannot be used as supplied, and a crosslinking treatment is required. Chitosan was crosslinked with glutaraldehyde by contact of chitosan with glutaraldehyde solution (10%, w/w). The volume of glutaraldehyde solution and the mass of chitosan were set to reach a 1:1 M ratio between the amine groups of the polymer and the aldehyde functions of the crosslinking agent. Finally, the particles were abundantly rinsed to remove traces of unreacted glutaraldehyde and dried at  $100^\circ\text{C}$ .

### Palladium sorption

The sorbent (1 g) was mixed for 24 h with a palladium solution (2 L) at a concentration of  $200 \text{ mg Pd L}^{-1}$  at pH 2. The solutions were then filtered and the residual concentration of palladium in the solution was measured using inductively coupled plasma atomic emission spectrometry (ICP-AES, Jobin-Yvon JY 2000, Longjumeau, France). The sorption capacity (amount of palladium adsorbed on the sorbent,  $q$ ,  $\text{mg Pd g}^{-1}$ ) was obtained by the mass balance equation.

### Procedure for palladium reduction

The reduction treatment consisted of bringing the loaded sorbent (200 mg) into contact with 100 mL of sulfuric acid solution (1% w/w) and 300 mg of zinc (provided as a fine powder). Since these drastic treatments can partially dissolve chitosan, it was necessary to measure the actual weight of the solid at the different stages in the synthesis process.

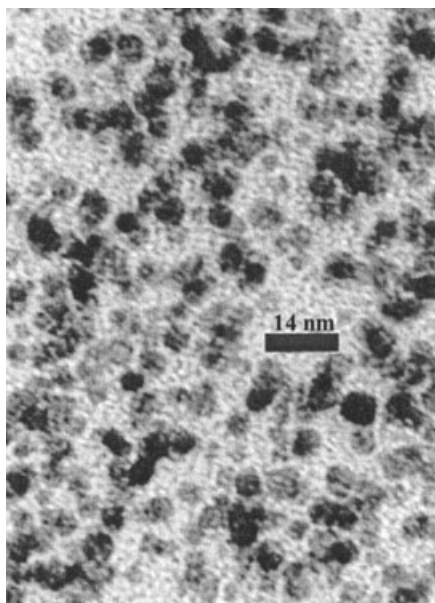


**Figure 1** TEM image of chitosan-supported palladium catalyst.

By taking into account the change in the weight of the solid during the sorption and reduction steps, it was possible to calculate the amount of palladium contained in the final product. Palladium content was close to  $105 \text{ mg Pd g}^{-1}$ . A digestion/mineralization procedure (contact of the catalyst with a hydrochloric acid and hydrogen peroxide mixture) was used to disrupt the polymer and dissolve the metal. ICP analysis confirmed the actual palladium content,  $102 \text{ mg Pd g}^{-1}$  catalyst in the standard PS1 particle size. For the study of particle size effect, other samples were specially prepared with higher concentrations of palladium in the loading bath. The same procedure was used for the determination of palladium content, giving 153, 144, 132, and  $124 \text{ mg Pd g}^{-1}$  for PS1 (and PS0, resulting from grinding and sieving of fraction PS1), PS2, PS3, and PS4, respectively.

### Characterization of the catalysts

Transmission electron microscopy (TEM) was used to measure the size of Pd nodules or crystals. Catalyst particles were incorporated in a liquid resin and, after crosslinking of the resin, thin slices of resin ( $60 \mu\text{m}$ ) were cut using a microtome. TEM observations showed that the size of metal crystals was close to 4–5 nm (Fig. 1). This is a critical parameter for catalytic activity: in most cases the smaller the size of the catalyst nodules, the greater the activity.<sup>36</sup> The particles were highly dispersed in the material although a slight gradient was observed between the center and the periphery of the particles. Some aggregates were also observed: agglomeration of small nodules led to the

formation of large palladium aggregates (around 30 nm).

X-ray photoelectron spectroscopy (XPS) analysis was also performed to determine the oxidation state of the palladium on the catalyst. It was shown that only 50 to 60% of palladium was reduced from Pd(II) to Pd(0).

### Procedure for nitroaniline degradation

4-Nitroaniline (4-NA) was degraded, unless otherwise specified, by contact of 5 mg of catalyst with 50 mL of a nitroaniline aqueous solution containing the organic compound at a concentration of  $25 \text{ mg L}^{-1}$  (approximately 0.18 mM) and sodium formate at a concentration of 25 mM. Experiments were performed at room temperature (i.e.,  $T = 20 \pm 1^\circ\text{C}$ ). The pH was initially controlled at pH 3 (unless specified) using a molar sulfuric acid solution. Samples were collected at selected contact times (ranging between 0 and 90 min) and filtered. A comparative experiment was performed using hydrogen gas as the hydrogen donor: the reactor containing the substrate (for which pH was controlled to pH 3) and the catalyst were first connected to a vacuum pump to remove air (and oxygen in the atmosphere of the reactor) and then hydrogen gas was flushed out for 10 s. Samples were regularly collected through a filtration system before analysis.

The filtrates were analyzed using a UV spectrophotometer (Varian 2050) to measure the absorbance of the solutions at 380 nm, after the sample (1-mL vol) had been acidified with  $20 \mu\text{L}$  of sulfuric acid solution (1% w/w). Acidification treatment allows the pH to be maintained at the same value for convenient determination of nitroaniline absorbance (that could change with the pH). This treatment results in a decrease of the intensity, compared to a nontreated sample, but it leads to reproducible analytical determinations. For the determination of reaction products (especially for Figs. 2 and 9) the samples were not acidified to prevent the masking of phenylenediamine (reaction product). Test experiments were performed to check the actual influence of the catalyst and hydrogen donor. In the absence of either hydrogen donor or catalyst, the reaction did not occur.

## RESULTS

### Characterization of decomposition products

Lauwiner et al. studied the reduction of aromatic nitro compounds with hydrazine hydrate using an iron oxide hydroxide catalyst and found that nitroaniline compounds were systematically converted into phenylenediamine compounds.<sup>37</sup> Xu et al. and Xi et al. investigated the hydrogenation of a series of aromatic nitro compounds using a palladium catalyst sup-

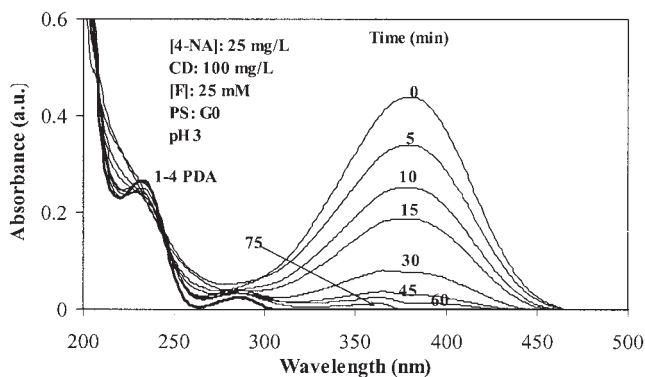


**Figure 2** UV-spectra of the solution during the hydrogenation reaction of 4-NA using a chitosan-supported palladium catalyst and sodium formate as the hydrogen donor, compared to the spectra of the substrate (4-NA) and final product (1,4-phenylenediamine, 1-4 PDA, bold line) catalyst ([F]: 25 mM; [4-NA]: 25 mg L<sup>-1</sup>; CD: 100 mg L<sup>-1</sup>; PS: 0–63 μm; numbers on the curves give contact times).

ported on vinylpyridine-based polymers. Nitroaniline compounds were systematically converted into phenylenediamine.<sup>38,39</sup> This kind of reaction is typically used for the production of phenylenediamine.<sup>40</sup> Xu et al. observed that the rate of hydrogenation of nitro compounds is strongly controlled by the structure of the substrate and more specifically to the type of substituent close to nitro moiety: electron-donating groups are more favorable for degradation than electron-withdrawing groups.<sup>38</sup> Amino and methoxy groups may increase the electron density of the nitro group, which in turn favors substrate coordination with palladium. Conversely, electron-withdrawing groups are not favorable to the activation of the nitro group. The reaction may be also controlled by steric effects. Hence, at low conversion the rate order was found to be  $p- > m- > o$ -substituted nitrobenzenes, while at higher conversion the rate order was  $p- > o- > m$ -substituted nitrobenzenes.<sup>38</sup>

Figure 2 shows the UV-spectra of the solution during the course of hydrogenation reaction compared to reference materials 4-NA and 1,4-phenylenediamine (1-4 PDA) in the presence of sodium formate. The fast disappearance of 4-NA was observed, while the presence of sodium formate in the solution masked the appearance of 1-4 PDA. However, at long contact time, the peak representative of 4-NA completely disappeared and new peaks at 235 and 287 nm appeared: these peaks represent 1-4 PDA in the presence of sodium formate at acidic pH.

### Influence of pH

The pH of the solution is a key parameter since it controls the adsorption of the reagents at the surface of the catalyst. Indeed, due to the acid–base properties

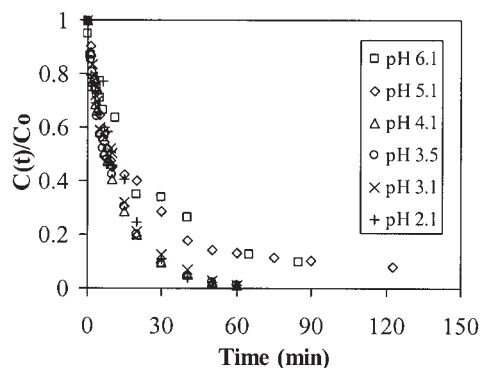
of chitosan, whose  $pK_a$  is close to 6.5, free amine groups of the polymer (nonsaturated with glutaraldehyde linkages or metal bonds) are protonated in acidic solutions. Hence, interactions of the catalytic supports with the hydrogen donor (i.e., sodium formate) are controlled by the electrostatic balance between the support and the reagent. Actually, the optimum pH conditions correspond to a moderate attraction of the reagent at the surface of the catalyst, while in the case of a strong interaction the reagent would saturate the surface of the catalyst, preventing desorption and access for substrate molecules.

Figure 3 shows the effect of the pH of the solution (varied between 2.1 and 6.1) on the degradation kinetics of 4-NA. In the range of pH 2.1 to 4.1, the curves perfectly overlapped and the substrate was completely degraded within the first 60 min of contact under selected experimental conditions. At pH 5.1 and 6.1, the curves overlapped and even after 2 h of contact 4-NA was not completely degraded: the degradation yield did not exceed 90%. At pH close to the  $pK_a$ , the protonation of chitosan was not complete and the attraction of formate anions was less efficient: the amount of formate anions sorbed at the surface of the catalyst may be rate limiting.

With weakly acidic solutions, pH variation (due to formate degradation and formation of carbon dioxide that buffered the solution) was significant. For this reason pH 3 was selected as the initial pH for further experiments, allowing the pH to be considered constant during the degradation operation.

### Influence of formate concentration

The concentration of the hydrogen donor is a critical parameter in these catalytic reactions.<sup>26,33</sup> A marked effect of sodium formate concentration was observed, especially at low reagent concentration (Fig. 4). In the 2.38–25 mM concentration range, the concentration of hydrogen donor was sufficient to completely degrade



**Figure 3** Influence of pH on 4-NA degradation on a chitosan-supported palladium catalyst ([F]: 25 mM; [4-NA]: 25 mg L<sup>-1</sup>; CD: 100 mg L<sup>-1</sup>; PS: 0–125 μm).

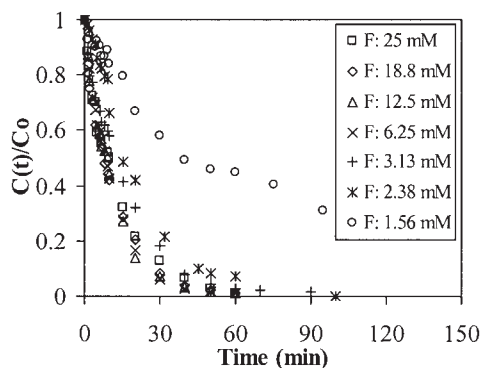


**Figure 4** Influence of formate concentration on 4-NA degradation on a chitosan-supported palladium catalyst (pH 3; [4-NA]: 25 mg L<sup>-1</sup>; CD: 100 mg L<sup>-1</sup>; PS: 0–125 μm).

the substrate. However, the time required to achieve the degradation increased with decreasing concentration of sodium formate. In the 6.25–25 mM concentration range, the curves overlapped perfectly and 50 min of contact was sufficient to completely degrade the nitroaniline. The required contact time was doubled when the concentration of hydrogen donor was decreased to 2.38 mM. When formate concentration was halved, to 1.56 mM, the degradation kinetics was significantly lowered and even after 2 h of contact, the degradation yield did not exceed 75%. The concentration of hydrogen donor controlled both the equilibrium, in the case of a lack of reagent, and the kinetics (at higher formate concentrations). It is interesting to observe that the minimum excess of sodium formate required for a complete degradation of 4-NA corresponded to a molar ratio F/4-NA of 13 (2.38 mM for the degradation of a nitroaniline concentration of 0.18 mM). This required excess (materialized by the formate/4-nitroaniline ratio, F/4-NA) was comparable to that obtained with nitrophenol, although it was shown to decrease with increasing reaction temperature.<sup>41</sup>

In the case of a large excess of hydrogen donor, the concentration of sodium formate can be considered constant throughout the degradation kinetics and the shape of the degradation kinetic curve is the typical shape of pseudo first-order kinetics.

$$\frac{dC(t)}{dt} = -k_0 C(t) \quad \text{or} \quad \ln \left[ \frac{C(t)}{C_0} \right] = -k_0 t, \quad (1)$$

where  $C_0$  and  $C(t)$  (mg L<sup>-1</sup>) are the initial substrate concentration and the concentration at time  $t$ , respectively. The parameter  $k_0$  (min<sup>-1</sup>) is the kinetic parameter for the first-order kinetic equation. Figure 5 shows some examples using this equation to model experimental results.

However, in some cases that will be discussed later, the apparent first-order equation failed to fit experi-

mental data and it was necessary to use the Langmuir–Hinshellwood equation.

When the data cannot be fitted using the simple first-order model, in the case of supported catalysis, Schüth and Reinhard use the following equation for modeling the kinetics:<sup>5</sup>

$$\frac{dC(t)}{dt} = \frac{-k_1 C(t)}{1 + k_2 C(t)}, \quad (2)$$

where  $k_1$  (min<sup>-1</sup>) and  $k_2$  (L mg<sup>-1</sup>) are the kinetic parameters.

This type of rate law is often observed for heterogeneous reactions in batch reactors with a constant volume and accounts for reactions that shift in order from zero to 1 as the substrate is utilized. Figure 5 (top) confirms that, at short contact times, the plot of the logarithm of the relative concentration versus time was not linear and became linear only when contact time increased (and the substrate was utilized). Integration of differential Eq. (2) gives the solution

$$t = \frac{1}{k_1} \left[ \ln \left[ \frac{C_0}{C(t)} \right] + k_2 (C_0 - C(t)) \right]. \quad (3)$$

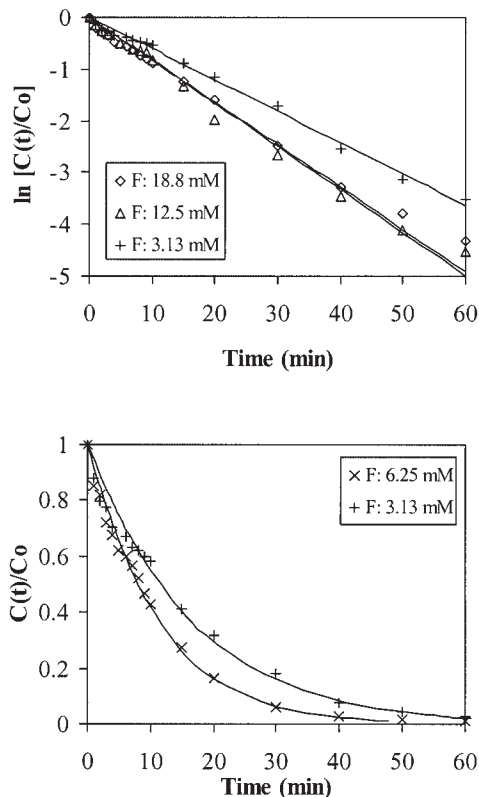


**Figure 5** Modeling of degradation kinetics (top: first-order equation plot—Eq. (1), bottom: variable order equation model—Eq. (2)). (pH 3; [4-NA]: 25 mg L<sup>-1</sup>; CD: 100 mg L<sup>-1</sup>; PS: 0–125 μm).

**TABLE I**  
Influence of Sodium Formate Concentration ([F], mM) on Kinetic Parameters for Nitroaniline Degradation ( $k_0$ ,  $\text{min}^{-1}$ ;  $k_1$ ,  $\text{min}^{-1}$ ;  $k_2$ ,  $\text{L mg}^{-1}$ )

[F]	$k_0 \cdot 10^2$	$k_1 \cdot 10^2$	$k_2 \cdot 10^2$
25	7.14	—	—
18.8	8.01	—	—
12.5	8.20	9.51	0.46
6.25	9.02	9.72	0.69
3.13	6.05	6.47	0.46
2.38	—	6.96	3.87

Kinetic parameters were determined using a nonlinear regression analysis tool. The first term (from the left of the right-hand side of the equation) represents a pseudo first-order kinetic equation, while the second term represents a zero-order kinetic equation. Figure 5 (bottom) shows the modeling of selected experimental data with Eq. (2).

Table I shows the kinetic parameters obtained from Eqs. (1) and (2) using a least-squares regression analysis to determine the parameters of the pseudo first-order equation and a nonlinear regression analysis (nonlinear regression tool with Levenberg–Marquardt algorithm in the Mathematica software package). The values of the kinetic parameters were of the same order of magnitude for concentrations ranging between 6.25 and 25 mM (between 0.07 and 0.09  $\text{min}^{-1}$ ). With decreasing formate concentration, the variable order equation fitted experimental data better. At very low formate concentration, the kinetic parameters  $k_1$  and  $k_2$  decreased.

#### Influence of 4-NA concentration

The degradation kinetics were hardly affected by the increase in initial nitroaniline concentration (Fig. 6). As expected, increasing the concentration of nitroaniline resulted in a slight increase in the time required to

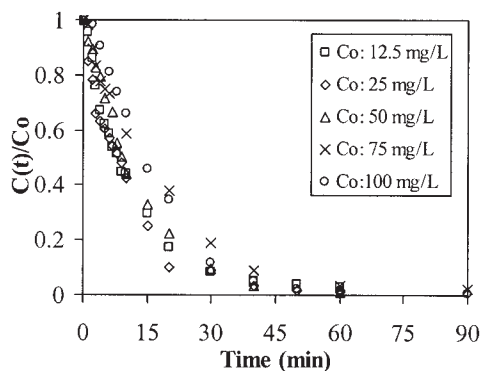


**Figure 6** Influence of nitroaniline concentration on 4-NA degradation on a chitosan-supported palladium catalyst (pH: 3; [F]: 25 mM; CD: 100  $\text{mg L}^{-1}$ ; PS: 0–125  $\mu\text{m}$ ).

**TABLE II**  
Influence of Nitroaniline Concentration ([4-NA],  $\text{mg L}^{-1}$ ) on Kinetic Parameters for Nitroaniline Degradation ( $k_0$ ,  $\text{min}^{-1}$ ;  $k_1$ ,  $\text{min}^{-1}$ ;  $k_2$ ,  $\text{L mg}^{-1}$ )

[4-NA]	$k_0 \cdot 10^2$	$k_1 \cdot 10^2$	$k_2 \cdot 10^2$
12.5	9.48	—	—
25	7.14	—	—
50	—	8.53	1.65
75	—	8.89	0.39
100	—	6.97	0.55

achieve complete degradation of the substrate. The formate concentration was set at 25 mM. This maintained an excess of hydrogen donor compared to substrate, which explains why the curves almost overlapped. Even with a 100  $\text{mg L}^{-1}$  concentration of nitroaniline, the molar ratio of F/4-NA was as high as 35, indicating a large excess of formate.

Table II gives the kinetic parameters. Below a nitroaniline concentration of 50  $\text{mg L}^{-1}$  the pseudo first-order equation fitted experimental data well. For nitroaniline concentrations of 50  $\text{mg L}^{-1}$  and above, the variable order model (Eq. 2) was more appropriate for the modeling of experimental data. The kinetic parameters  $k_0$  and  $k_1$  hardly varied between 7 and 9.5  $\text{min}^{-1}$ . Parameter  $k_1$  is analogous to parameter  $k_0$  for systems in which parameter  $k_2$  (and  $k_2C$ ) are negligible. Although the comparison of the values for  $k_0$  and  $k_1$  is not fully acceptable, it gives a preliminary indication of the trend in the variation of kinetic rate. The concentration of nitroaniline did not significantly affect the degradation rate under the selected experimental conditions, with an excess of hydrogen donor.

#### Influence of catalyst particle size

The size of catalyst particles was varied to test the influence of diffusion mechanisms on the control of degradation rates. Figure 7 shows that this parameter

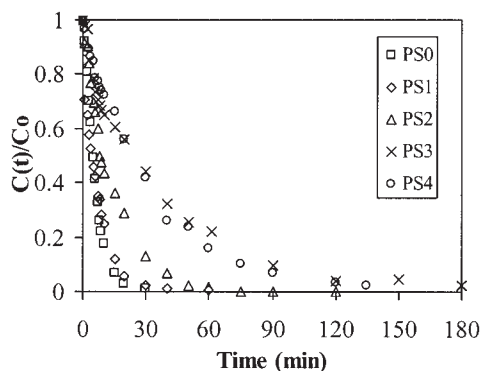


**Figure 7** Influence of catalyst particle size on 4-NA degradation on a chitosan-supported palladium catalyst (pH: 3; [F]: 25 mM; [4-NA]: 25  $\text{mg L}^{-1}$ ; CD: 100  $\text{mg L}^{-1}$ ).

**TABLE III**  
**Influence of Catalyst Particle Size on Kinetic Parameters for Nitroanaline Degradation ( $k_0$ ,  $\text{min}^{-1}$ )**

Particle size ( $\mu\text{m}$ )	$k_0 \cdot 10^2$
0–63	17.26
0–125	13.50
125–250	7.14
250–500	2.71
500–710	2.89

had a significant effect on the kinetic rate but did not influence the conversion yield. The curves for PS0 and PS1 catalysts superimposed perfectly. For a size of catalyst particle in the range 0–125  $\mu\text{m}$  the diameter of the particle did not affect the kinetics of the reaction. A similar conclusion can be reached in the case of PS3 and PS4 catalysts. However, in this case the kinetics were significantly slower. Hence, 4–5 min of contact was sufficient to halve the initial concentration in the case of PS0 and PS1 catalysts while the half-reaction time (HRT) reached 25 min for PS3 and PS4 catalysts. The PS2 catalyst had intermediate behavior: the HRT was close to 8 min. Similar results were obtained in the case of chlorophenol dehalogenation and nitrophenol degradation using the same catalyst.<sup>33,34</sup> The positive effect of size decrease may be explained by several reasons: (a) increase of palladium loading (see Experimental), (b) increase of external surface area, (c) limitation of diffusion restrictions.

The impact of catalyst loading is relatively limited. Indeed, previous studies performed with the same catalyst on nitrophenol degradation showed that the catalytic activity was only slightly varied by increasing palladium loading: palladium is more efficiently used at low metal loading. The increase of external surface area usually controls mass transfer through the film around catalyst particles. Decreasing particle size is thus expected to increase degradation kinetics. Decreasing particle size has a significant effect on the resistance to intraparticle mass transfer, especially in the case of low-porosity materials. Chitosan is characterized as a weakly porous material so the diffusion of solute molecules to the center of the particle may be a critical parameter.

By analogy with adsorption processes,<sup>42</sup> the kinetic rate is expected to vary with the reciprocal of particle radius in the case of systems controlled by film diffusion and with the reciprocal of the square of particle radius for systems controlled by intraparticle diffusion. Table III reports on the kinetic parameter  $k_0$  for varying size of catalyst particles. The correlation of the kinetic rate with the reciprocal of both particle radius and square particle radius was checked. None of these correlations gave a convincing trend. It is possible to suggest that both external and intraparticle diffusion resistance controlled the kinetic rate.

Alternatively, it is also possible to suggest that the reaction was limited to the external surface of the catalyst or to thin external layers of the particles and that the internal palladium crystals did not significantly contribute to the reaction. This would explain why palladium was more efficiently used with low palladium-loaded particles, as previously cited. In this case, the maximum thickness to be respected for the optimum use of palladium on the support would be close to 60–70  $\mu\text{m}$ . TEM analysis showed that the distribution of palladium crystals was denser at the periphery of the particle. It is also possible that the reduction of palladium during the preparation of the catalyst may be less efficient at the center of the particle. Although the distribution of palladium is expected to be homogenous through the particle with saturation of the sorbent as shown in previous works,<sup>43,44</sup> the slight differences observed may be due to short contact times not sufficient to achieve equilibrium and saturation of the sorbent. Additionally, the size of catalyst particles may affect the ability of Pd immobilized in the central part of catalyst particles to be reduced. This may contribute to increase the heterogeneity of the catalyst and improve the impact of this experimental parameter.

#### Influence of catalyst dosage

The catalyst dosage (CD) was varied around the reference value (i.e., CD: 100  $\text{mg L}^{-1}$ ) to check whether this experimental parameter affects the initial or final section of the kinetic curves. Figure 8 shows that the curves overlapped in the first section of the curve (up to a contact time of 5 min) that is usually controlled by external film diffusion, while the second section of the curve was significantly influenced by catalyst dosage. While 90 minutes were necessary to achieve 4-NA degradation at low catalyst dosage (i.e., CD: 50  $\text{mg L}^{-1}$ ), the end of the degradation kinetics was reached after 60 min and 30 of contact time for CD: 100  $\text{mg L}^{-1}$

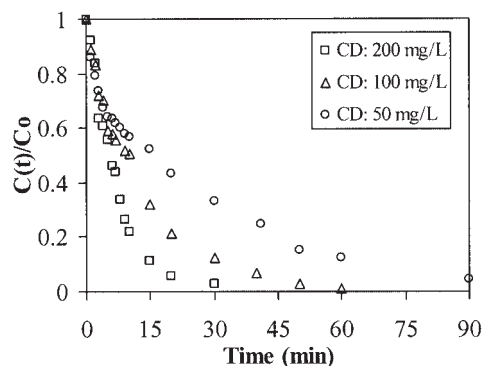


**Figure 8** Influence of catalyst dosage on 4-NA degradation on a chitosan-supported palladium catalyst (pH: 3; [F]: 25 mM; [4-NA]: 25  $\text{mg L}^{-1}$ ; PS: 0–125  $\mu\text{m}$ ).

**TABLE IV**  
Influence of Catalyst Dosage (CD, mg L<sup>-1</sup>) on Kinetic Parameters for Nitroaniline Degradation ( $k_0$ , min<sup>-1</sup>)

CD	$k_0 \cdot 10^2$
50	3.45
100	7.14
200	14.11

and CD: 200 mg L<sup>-1</sup>, respectively. Similar variations were observed with the HRT: 17, 10, and 5–6 min for CD: 50 to 200 mg L<sup>-1</sup>. Kinetic parameter  $k_0$  varied linearly with catalyst dosage as shown in Table IV.

Since the initial slope of the curve was not affected by the increase in catalyst dosage, we can suspect that the reaction was not being controlled by external diffusion: the increase in external surface area increased with catalyst dosage. This could confirm that the reaction only occurs in the first external layers of the particle (thickness evaluated to be 60–70  $\mu\text{m}$  from the results obtained at different particle sizes). The limitations due to diffusion in the first layers of the catalyst particles were compensated by the increase in the number of available palladium crystals at the external surface of the catalyst (as a result of the increase in catalyst dosage).

#### Influence of the type of hydrogen donor

To evaluate the impact of the type of hydrogen donor as seen in Figure 9, the kinetic profiles for the degradation of 4-NA with Pd-supported catalyst were operated using hydrogen gas (at the pressure of 1 bar) under similar experimental conditions as those selected for Figure 2. Using hydrogen gas as the hydrogen donor allows the kinetics of degradation to be increased substantially. Basically, the time required for achieving the degradation of the substrate was halved when sodium formate was substituted with hydrogen gas, while with sodium formate 60 to 75 min was necessary for achieving the complete degradation of 4-NA (at the concentration of 25 mg L<sup>-1</sup>): after 30 min of reaction 4-NA was fully converted into 1–4 PDA. Preliminary experiments (not shown) clearly indicated that the kinetics of the hydrogenation process depended on the interfacial surface between the gas phase and the liquid phase. Hydrogen transfer to the liquid phase revealed a limiting step.

#### CONCLUSION

Chitosan proved to be a suitable support for the immobilization of palladium in the manufacture of palladium-based catalysts. The high sorption capacity, the stability of palladium on the sorbent over a wide range of pH, and the versatility of the material (chem-

ical modifications, physical conditioning in the form of membranes, fibers, hollow fibers) justify the use of this biopolymer for the preparation of supported catalysts. Tested on nitroaniline degradation the catalyst was very efficient at degrading this organic contaminant using sodium formate as the hydrogen donor. Optimum degradation occurred at pH close to 3. Formate must be in excess to allow complete nitroaniline degradation and optimum degradation kinetics were obtained when the molar ratio F/4-NA was greater than 13. Maintaining this required excess of hydrogen donor enables complete degradation of nitroaniline over a large concentration range. The catalyst dosage and size of catalyst particles are important experimental parameters. The reaction appears to be limited to external layers of the particles. Hence, decreasing the particle size or increasing the catalyst dosage significantly improved degradation kinetics.

These results must be considered a demonstration of the possibility of using chitosan as a support for heterogeneous catalysis. Although catalytic performance should be increased to be competitive with conventional materials, these preliminary data serve to identify the limiting parameters of the process and the critical characteristics of the catalyst. The challenge for the development of chitosan-supported Pd-catalysts is clearly the control of diffusion properties (and appropriate polymer conditioning) and the control of Pd reduction efficiency. Increasing the percentage of Pd reduced to the metal state will result in a significant increase of its reactivity. Another method for improving catalytic activity consists of using hydrogen gas as the hydrogen donor.

The dramatic effect of particle size can be minimized using appropriate conditioning of the polymer. Hollow chitosan fibers were therefore prepared,<sup>45</sup> this

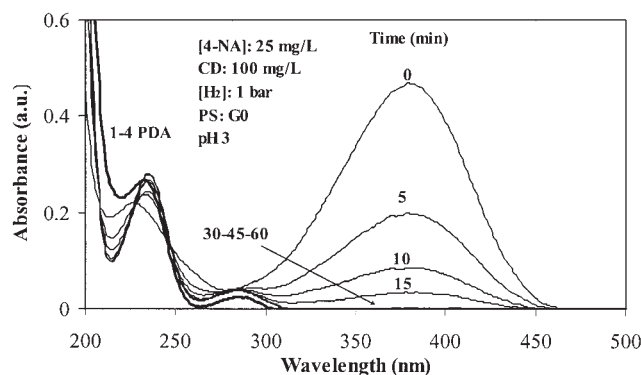


**Figure 9** UV-spectra of the solution during the hydrogenation reaction of 4-NA using a chitosan-supported palladium catalyst and hydrogen gas as the hydrogen donor, compared to the spectra of the substrate (4-NA) and final product (1,4-phenyldiamine, 1–4 PDA, bold line) catalyst P(H<sub>2</sub>): 1 bar; [4-NA]: 25 mg L<sup>-1</sup>; CD: 100 mg L<sup>-1</sup>; PS: 0–63  $\mu\text{m}$ ; numbers on the curves give contact times.



support having recently been used for palladium immobilization and the preparation of a new catalytic system (after appropriate chemical reduction). Hollow catalytic fibers can be used for similar reactions: with solutions being flowed through the lumen of the fiber, while the hydrogen donor is circulated outside the fiber. Sodium formate and hydrogen gas were successfully used as hydrogen donors for the degradation of nitrophenol using these catalytic chitosan-made hollow fibers.<sup>35</sup>

The authors thank the ANVAR (Agence Nationale de Valorisation de la Recherche) for financial support for the Chito/Cat project.

## References

1. Gawdzik, B.; Matynia, T. *J Chromatogr A* 1996, 733, 491.
2. Spacek, W.; Bauer, R.; Heisler, G. *Chemosphere* 1995, 30, 477.
3. Benz, M.; Prins, R. *Appl Catal A Gen* 1999, 183, 325.
4. Macquarrie, D. J.; Gotov, B.; Toma, S. *Platinum Metals Rev* 2001, 45, 102.
5. Schüth, C.; Reinhard, M. *Appl Catal B Environ* 1998, 18, 215.
6. Gallezot, P.; Laurain, N.; Isnard, P. *Appl Catal B Environ* 1996, 9, 11.
7. Choudhary, V. R.; Sane, M. G.; Tambe, S. S. *Ind Eng Chem Res* 1998, 37, 3879.
8. Gao, H.; Xu, Y.; Liao, S.; Yu, D. *React Polym* 1994, 23, 113.
9. Patel, D. R.; Ram, R. N. *J Mol Catal A Chem* 1998, 130, 57.
10. Ford, W. T. *React Funct Polym* 2001, 8, 3.
11. Drelinkiewicz, A.; Hasik, M. *J Mol Catal A Chem* 2001, 177, 149.
12. Augustine, R. L.; Tanielyan, S. K. *J Mol Catal A Chem* 1996, 112, 93.
13. Altava, B.; Burguete, M. I.; García-Verdugo, E.; Luis, S. V.; Vicent, M. J.; Mayoral, J. A. *React Funct Polym* 2001, 48, 125.
14. Baiker, A. *J Mol Catal A Chem* 1997, 115, 473.
15. Pispisa, B.; Venanzi, M.; Palleschi, A. *J Chem Soc Faraday Trans* 1994, 90, 435.
16. Yashima, E. *J Chromatogr A* 2001, 906, 105.
17. Haginaka, J. *J Chromatogr A* 2001, 906, 252.
18. Felix, G. *J Chromatogr A* 2001, 906, 171.
19. Malinowska, I.; Rózyłó, J. K. *Biomed Chromatogr* 1997, 11, 272.
20. Chiessi, E.; Pispisa, B. *J Mol Catal* 1994, 87, 177.
21. Jin, J.-J.; Chen, G.-C.; Huang, M.-Y.; Jiang, Y.-Y. *React Polym* 1994, 23, 95.
22. Han, H.-S.; Jiang, S.-N.; Huang, M.-Y.; Jiang, Y.-Y. *Polym Adv Technol* 1996, 7, 704.
23. Zeng, X.; Zhang, Y.; Shen, Z. *J Polym Sci A Polym Chem* 1997, 35, 2177.
24. Yin, M.-Y.; Yuan, G.-L.; Wu, Y.-Q.; Huang, M.-Y.; Jiang, Y.-Y. *J Mol Catal A Chem* 1999, 147, 93.
25. Quignard, F.; Choplin, A.; Domard, A. *Langmuir* 2000, 16, 9106.
26. Vincent, T.; Guibal, E. *Ind Eng Chem Res* 2002, 41, 5158.
27. Buisson, P.; Quignard, F. *Austr J Chem* 2002, 55, 73.
28. Arena, B. J. *Hydrogenation Using Chitin and Chitosan Based Immobilized Metal Catalysts*; U.S. Patent; 4,431,836, February 14, 1984.
29. Guibal, E.; Vincent, T.; Larkin, A.; Tobin, J. M. *Ind Eng Chem Res* 1999, 38, 4011.
30. Ruiz, M.; Sastre, A.; Guibal, E. *React Funct Polym* 2000, 45, 155.
31. Guibal, E.; Milot, C.; Roussy, J. *Sep Sci Technol* 2000, 35, 1021.
32. Guzman, J.; Saucedo, I.; Revilla, J.; Navarro, R.; Guibal, E. *Langmuir* 2002, 18, 1567.
33. Vincent, T.; Spinelli, S.; Guibal, E. *Ind Eng Chem Res* 2003, 42, 5968.
34. Vincent, T.; Guibal, E. *Langmuir* 2003, 19, 8475.
35. Guibal, E.; Vincent, T. *Environ Sci Technol* 2004, 38, 4233.
36. Mabbett, A. N.; Yong, P.; Baxter-Plant, V. S.; Mikheenko, I. P.; Farr, J. P. G.; Macaskie, L. E. In *Biohydrometallurgy: Fundamentals, Technology and Sustainable Development*, Ciminelli, V. S. T.; Garcia Jr., O., (Eds.); Wiley: Amsterdam, 2001; pp. 335–342.
37. Lauwiner, M.; Rys, P.; Wissman, J. *Appl Catal A Gen* 1998, 172, 141.
38. Xu, S.; Xi, X.; Shi, J.; Cao, S. *J Mol Catal A Chem* 2000, 160, 287.
39. Xi, Y.; Liu, Y.; Shi, J.; Cao, S. *J Mol Catal A Chem* 2003, 192, 1.
40. Joo, Y. J.; Kim, J. E.; Won, J. I. *Method of Preparing p-Phenylenediamine*; U.S. Patent; 6,245,943, June 12, 2001.
41. Guibal, E.; Vincent, T. *J Environ Manage* 2004, 71, 97.
42. Helfferich, F. *Ion Exchange*; Dover: Mineola, NY, 1995.
43. Guibal, E.; Vincent, T.; Navarro Mendoza, R. *J Appl Polym Sci* 2000, 75, 119.
44. Guibal, E.; Von Offenbergsweeney, N.; Vincent, T.; Tobin, J. M. *React Funct Polym* 2002, 50, 149.
45. Vincent, T.; Guibal, E. *Ind Eng Chem Res* 2001, 40, 1406.